

# Surface effects on hydrodynamic evolution

Sanatan Digal<sup>1,2,\*</sup> and P.S. Saumia<sup>3,†</sup>

<sup>1</sup>*The Institute of Mathematical Sciences, Chennai, 600113, India*

<sup>2</sup>*Homi Bhabha National Institute, Training School Complex,  
Anushakti Nagar, Mumbai 400085, India*

<sup>3</sup>*Bogoliubov Laboratory of Theoretical Physics, JINR, 141980 Dubna, Russia*

## Abstract

We study the effect of surface tension of the phase boundary in the dynamics of an expanding fluid. A fluid at local thermal equilibrium, but has a slowly varying temperature profile, like the plasma formed in heavy ion collisions, will have rapidly varying order parameter field at the edge of the plasma where the temperature falls below the transition temperature. In the case where the free energy admits a first order transition, the gradient energy of this field will act as surface tension. We couple hydrodynamics and order parameter field evolutions to study the effect of this surface in the expansion of the plasma. We see that the surface slows down the expansion which reflects in the development of radial flow and momentum anisotropy.

---

\* [digal@imsc.res.in](mailto:digal@imsc.res.in)

† [saumia@theor.jinr.ru](mailto:saumia@theor.jinr.ru)

## I. INTRODUCTION

Heavy ion collision experiments provide us with a way to study the properties of strongly interacting matter at extreme conditions. One of the important observations from high energy heavy ion collisions is the collective flow. It indicates that the matter formed at these collisions reach thermodynamic equilibrium rapidly and evolves as a fluid, expand and cool down. Subsequently the constituent particles freeze out before reaching the detectors. The various stages of the evolution can be indirectly observed from the flow of different particles that freeze out at different times. The high energy collisions at RHIC and LHC creates matter in the deconfined regime at high temperatures and very small baryon densities. Lattice studies suggest that the transition from deconfinement to confinement of strongly interacting matter at these conditions is a cross over [1]. Various theoretical models predict a critical end point followed by a first order transition line at higher baryon densities [2]. There are attempts to study higher baryon density regimes at experiments like FAIR and NICA and one expects to see some indications of a first order phase transition at these experiments [3, 4].

There have been several approaches to understand the dynamics of the quark gluon plasma formed in heavy ion collisions. Hydrodynamics with an appropriate equation of state has been successful in explaining the flow observables at RHIC and LHC [5, 6]. There also are attempts to understand the dynamics of the phase transitions as well as the possibility of formation of center domains and topological defects using the evolution of order parameter fields using different effective field theory models [7–10]. First order phase transition dynamics has also been studied by reducing the hydrodynamics equations into equations for order parameter of the system in the vicinity of the critical point [11]. But even when the system is well in the deconfined region, in heavy ion collisions, the system will have a spatial profile of temperature slowly varying away from the centre to zero towards the edges. Hence the system at all times after thermal equilibration should have a phase boundary until it cools down below the transition temperature. This means that the order parameter at this boundary will rapidly vary from deconfinement to confinement value and the order parameter field will have a gradient energy. In the case of a first order equation of state, this gradient energy will always be finite and will act as surface tension. The radial expansion of the plasma in this case should feel a resistance since increasing the surface area of the

system increases the surface energy. Intuitively, then it suggests that the system with a phase boundary should have a constrained radial expansion compared to a system without a phase boundary.

Hydrodynamics alone, even with a first order equation of state, cannot address surface tension effects at the boundary. Effective field theory with an appropriate order parameter, on the other hand, can be used to study the evolution of the phase boundary where the effect of surface tension is automatically taken care of, but cannot be used to study collective flow. Hence, in this work, we attempt to couple these two together, a fluid in the bulk with a surface which is represented by the gradient energy of an order parameter field. The evolution of the coupled system is expected to handle the surface effects on the flow of the fluid. We would like to clarify that we do not study the dynamics of the phase transition of the system through bubble nucleation here. Our system is in the deconfined region but it has a boundary across which the temperature falls below the transition temperature and hence has a surface.

In section II, we discuss the formulation of the problem and explain the Polyakov loop model which is used for the evolution of order parameter here. In section III, the equation of state and initial conditions are explained along with the implementation of the techniques used to numerically solve the partial differential equations. Section IV discusses the results which show the effects of phase boundary on the development of radial flow as well as momentum anisotropy of the fluid and section V summarizes the study.

## II. COUPLING THE POLYAKOV LOOP FIELD TO THE FLUID

To begin with, let us assume that we have two systems interacting with each other, one is the fluid and the other is an order parameter field. Then the evolution of the system is governed by the conservation of the energy momentum tensor of the combined system. This should be supplemented by an equation of state for the fluid as well as an equation of motion for the evolution of the order parameter field. For confinement deconfinement transition, Polyakov loop  $\phi$  is a good order parameter. For simplicity, we assume that the fluid is quark less. Then we can use a Polyakov loop effective field theory model for the equation of state as well as for the dynamics of the order parameter part the system. We use the model by Pisarski [12–14] which has a potential with a weak first order transition. Thus the equations

we need to solve are:

$$\partial_\mu T^{\mu\nu} = 0 \quad (1)$$

and

$$\frac{\partial^2 \phi}{\partial t^2} - \nabla^2 \phi = -\frac{\partial V(\phi, T)}{\partial \phi} \quad (2)$$

where

$$T^{\mu\nu} = T_{fluid}^{\mu\nu} + T_\phi^{\mu\nu} \quad (3)$$

Eq. (2) describes the evolution of the order parameter field given an initial condition [15].

$T_{fluid}^{\mu\nu}$  is the energy-momentum tensor of the fluid given by

$$T_{fluid}^{\mu\nu} = (\epsilon + p)u^\mu u^\nu + p\eta^{\mu\nu} \quad (4)$$

with  $\epsilon$  and  $p$  the energy density and pressure density of the fluid,  $u^\mu = \gamma(1, \vec{v})$  the 4-velocity and  $\eta^{\mu\nu}$  the Minkowski metric with signature  $(- + + +)$ .  $\vec{v}$  is the 3-velocity of the fluid element and  $\gamma$  is the corresponding Lorentz factor given by  $\gamma = \frac{1}{\sqrt{1-\vec{v}^2}}$ .  $T_\phi^{\mu\nu}$  is the energy-momentum tensor of the Polyakov loop field  $\phi$  and  $V(\phi, T)$  is the effective potential at temperature  $T$  given by

$$V(\phi, T) = b_4 T^4 \left[ -\frac{b_2(T)}{4} \phi^2 - \frac{b_3}{6} \phi^3 + \frac{1}{16} \phi^4 \right]. \quad (5)$$

Note that the Polyakov loop field is usually written as a complex scalar field and the potential should be written as a function of  $\phi$  and  $\bar{\phi}$ . But here we ignore fluctuations of the order parameter field and assume that the imaginary component of the field is not excited or remains small during the evolution. Thus we can write  $\bar{\phi} = \phi$  and that simplifies our implementation. The above effective potential Eq.(5) with the following form of  $b_2(T)$

$$b_2(T) = (1 - 1.11 T_c/T) (1 + 0.265 T_c/T)^2 (1 + 0.3 T_c/T)^3 - 0.487 \quad (6)$$

and the coefficients  $b_3 = 2.0$  and  $b_4 = 0.6016$  reproduces the pressure of the pure gauge theory computed from non-perturbative lattice method(s) and is given by  $p = -V(\phi, T)$ .  $T_c$  is the transition temperature.

Since the order parameter field is a scalar field, the corresponding energy-momentum

tensor can be calculated as follows. The Lagrangian of the field is given by

$$L(\phi, T) = \alpha T^2 \partial_\mu \phi \partial^\mu \phi - V(\phi, T) \quad (7)$$

The corresponding energy-momentum tensor is given by

$$T_\phi^{\mu\nu} = \frac{\delta L}{\delta(\partial_\mu \phi)} - \eta^{\mu\nu} L \quad (8)$$

After doing the variation of the Lagrangian,  $T^{\mu\nu}$  can be written as

$$T_\phi^{\mu\nu} = 2\alpha T^2 \partial^\mu \phi \partial^\nu \phi - \eta^{\mu\nu} (\alpha T^2 \partial_\beta \phi \partial^\beta \phi - V(\phi, T)) \quad (9)$$

$\alpha$  is a constant given by  $2N/g^2$  [13], where  $N$  is the number of colors and  $g$  is the gauge coupling constant. For  $g/4\pi = 0.3$ ,  $\alpha = 1.6$ .

Let us look at Eqs. (1) and (2) again. Even though we need to solve these two equations together, the fluid part with variables like energy density, pressure and 4-velocities seems almost uncoupled to the Polyakov loop field part which only has the field variable. But there is a mechanism of feedback between these two systems and that is through the temperature of the fluid. The Polyakov loop effective potential is a function of temperature and hence the field evolution in Eq.(2) will depend on the local temperature which is determined by the fluid parameters  $\epsilon$  and  $p$  via the equation of state which in turn can be written down from the effective model.

Lattice results are used to estimate the thermodynamic variables of the Polyakov loop field at a certain temperature and these variables are equated with that of the fluid for hydrodynamic simulations. Similarly using Polyakov loop model, at thermodynamic equilibrium, pressure of the fluid is estimated as  $-V(\phi, T)$  at the given temperature. So if the field is at the minimum of the potential, adding up the pressure of the fluid and  $-V(\phi, T)$  in  $T^{\mu\nu}$  leads to double counting. Note that even though fluid pressure can be obtained from the free energy of the Polyakov loop, the evolution of the fluid and the Polyakov loop field are very different. For example, the evolution of the Polyakov loop field hardly shows any flow. This is because, Polyakov loop captures only the low momentum modes of the system as it is a condensate field.

If we look at Figs. 1 and 2, we can see that the value of the field differs from its value

at the minimum only near the surface. Here the field interpolates between its value at confinement (which is zero) to its value at deconfinement at the transition. So assuming local thermal equilibrium, we consider only the fluid pressure and neglect the contribution of the potential  $V(\phi, T)$  in  $T_\phi^{\mu\nu}$ . Thus the only non-zero term in  $T_\phi^{\mu\nu}$  is the gradient energy at the surface and this serves as surface tension at the phase boundary. Since the field is away from its minimum at the surface due to gradients,  $-V(\phi, T)$  will not be same as the pressure of the fluid here. It is not clear how to calculate the energy momentum tensor of the field in this case. One could write down the pressure contribution from the field as equal to the difference between the equilibrium value and the value of the field profile, ie,  $-(V(\phi, T) - V_{eq}(\phi, T))$  where  $V_{eq}(\phi, T)$  corresponds to the minimum value of the free energy at a given temperature. This will make sure that it remains zero everywhere except at the phase boundary. Effectively, this is what we are doing by neglecting the effective potential contribution in the energy momentum tensor of the Polyakov loop field, except at the surface. But at the boundary even if this difference remains negligible compared to the gradient term, it gives a negative contribution to the total pressure and it leads to numerical errors. Hence in the results presented, this term is ignored in  $T_\phi^{\mu\nu}$  and only gradient term is considered.

### III. IMPLEMENTATION

#### A. Equation of state

Using thermodynamic relations, the energy density can be calculated from the free energy as,

$$\epsilon = -T \left( \frac{\partial V(\phi, T)}{\partial T} \right)_{\text{volume}=\text{constant}} + V(\phi, T) \quad (10)$$

Minimizing the effective potential (5) with respect to  $\phi$  and using the corresponding field value at the given temperature, the energy density and pressure can be calculated. This gives the equation of state for the fluid. Fig. 1(a) shows the order parameter as a function of temperature and Fig. 1(b) shows the variation of energy density ( $\epsilon/T^4$ ) and pressure ( $p/T^4$ ). In this model, the order parameter is zero below the transition temperature and as a result the pressure remains zero in the confined phase. There are several problems because

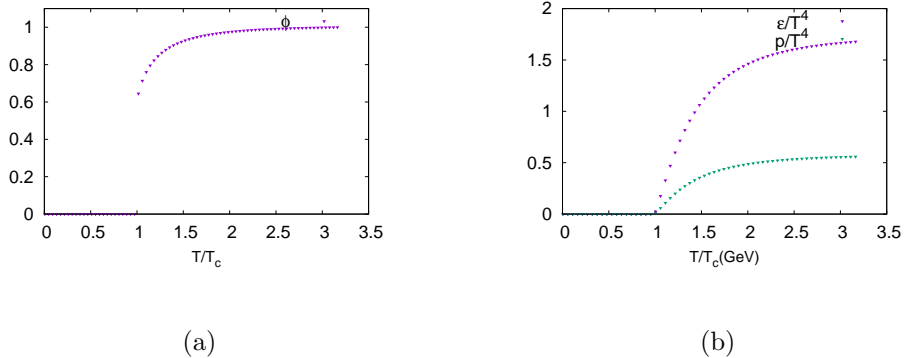


FIG. 1. Equation of state

of this when we try to evolve the fluid using this equation of state. These problems will be discussed later in detail.

### B. Reduction into 2D and initial conditions

We don't consider Bjorken expansion along the longitudinal axis. Here we have a system with a first order transition. First order phase transitions are expected at low temperatures and high baryon densities for which Bjorken flow component will be small. So for central collisions, we have a spherical system of expanding fluid and for non-central collisions, we have an ellipsoid. For simplicity we assume that our system has an azimuthal symmetry. Then we can reduce the system into 2+1 dimensions and use cylindrical co-ordinates to solve Eqs. (1) and (2). The equation of motion for the order parameter (2) then reduces to

$$\frac{\partial^2 \phi}{\partial t^2} - \frac{\partial^2 \phi}{\partial r^2} - \frac{1}{r} \frac{\partial \phi}{\partial r} - \frac{\partial^2 \phi}{\partial z^2} = - \frac{\partial V(\phi, T)}{\partial \phi} \quad (11)$$

We assume simple Gaussian initial conditions along  $r$  and  $z$  for the initial energy density of the fluid. For non-central collisions, the initial conditions require different widths for the initial Gaussian along  $r$  and  $z$ . The major axis of the ellipsoid is along  $z$  in cylindrical coordinate system, so the width along  $z$  will be larger. Using the equation of state, the initial pressure and temperature profiles are obtained. The initial  $\phi$  field is obtained by evolving Eq.(11) with this initial temperature profile fixed. We use a small dissipation term for the Polyakov loop field so that it settles into the minimum of the potential. In the absence of dissipation, the field tends to oscillate around the minimum. No matter what

initial profile is chosen, Eq.(11) along with dissipation evolves it into the one which minimizes the energy with respect to the given temperature profile. Fig. 2 shows this input Polyakov loop profile for the coupled system with the corresponding temperature profile.

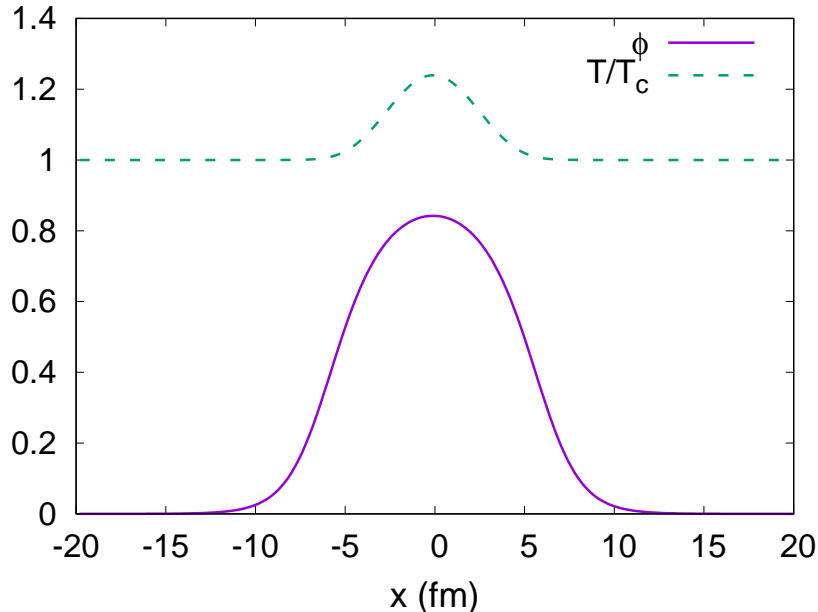


FIG. 2. Initial temperature and Polyakov field profile for the coupled system along x-axis.

We have seen earlier that energy density and pressure of the Polyakov loop field are zero outside the deconfined region for our equation of state. This means that the initial Gaussian profile of energy density cannot go to zero at large radii. Any non-zero value below the value of the energy density at transition temperature is unphysical. Thus we let the Gaussian at large radii go to the value of  $\epsilon$  at the transition temperature. But in order to have a phase boundary, we need a confined phase outside and this is ensured from the fact that the order parameter is zero in that region.

### C. Solving the PDEs

The conservation equations 1 are rewritten by separating the fluid and the field parts as

$$\partial_\mu T_{fluid}^{\mu\nu} = -\partial_\mu T_\phi^{\mu\nu} \quad (12)$$



We use Kurganov-Tadmor scheme [16, 17] on the fluid part of the conservation equation (12) which turns it into a set of ordinary differential equations and use a second order Runge-Kutta method to solve it numerically as in [17]. Here we only quote the final equations of the scheme in one spatial dimension. For more than one dimension, the scheme is repeated in each of them. If we have a conservation equation in one spatial dimension and is given by

$$\partial_t u = -\partial_x f \quad (13)$$

where  $f$  can be written as  $f = vu$ , the final result in the  $\Delta t \rightarrow 0$  limit of this equation can be written as a conservation equation of the cell average

$$\bar{u}(t) = \frac{1}{\Delta x} \int_{x_{j-1/2}}^{x_{j+1/2}} dx u(x, t) \quad (14)$$

and is given by

$$\frac{d\bar{u}(t)}{dt} = -\frac{F_{j+1/2}(t) - F_{j-1/2}(t)}{\Delta x} \quad (15)$$

where

$$\begin{aligned} F_{j\pm 1/2} = & \frac{f_{j\pm 1/2,+}(t) + f_{j\pm 1/2,-}(t)}{2} \\ & - \frac{a_{j\pm 1/2}(t)}{2} (\bar{u}_{j\pm 1/2,+}(t) - \bar{u}_{j\pm 1/2,-}(t)) \end{aligned} \quad (16)$$

The subscripts  $j \pm 1/2$  denote points in space separated by  $\Delta x/2$  from the point  $j$ . Here  $a$  is the maximum propagation speed given by  $|\partial f/\partial u|$  and  $f_{j\pm 1/2,\pm}$  is calculated from

$$\bar{u}_{j+1/2,+} = \bar{u}_{j+1} - \frac{\Delta x}{2} (u_x)_{j+1} \quad (17)$$

$$\bar{u}_{j-1/2,-} = \bar{u}_j + \frac{\Delta x}{2} (u_x)_j \quad (18)$$

$(u_x)_j$  is the spatial derivative and is determined by the minmod flux limiter which is given by

$$(u_x)_j = \text{minmod} \left( \theta \frac{\bar{u}_{j+1} - \bar{u}_j}{\Delta x}, \theta \frac{\bar{u}_{j+1} - \bar{u}_{j-1}}{2\Delta x}, \theta \frac{\bar{u}_j - \bar{u}_{j-1}}{\Delta x} \right) \quad (19)$$

where

$$\text{minmod}(x_1, x_2, \dots) = \begin{cases} \min x_j, & \text{if } x_j > 0 \forall j \\ \max x_j, & \text{if } x_j < 0 \forall j \\ 0, & \text{otherwise} \end{cases} \quad (20)$$

$\theta$  is a parameter that controls the numerical diffusion and oscillation and we choose  $\theta = 1.1$  [17].

Now Eq.(15) can be solved using an ODE solver. We use Heun's method to solve this and the steps for an equation of the form

$$\frac{du}{dt} = F(t) \quad (21)$$

are as follows:

$$\text{Heun's : } \begin{cases} u^{(1)} = u^n + \Delta t F(t, u^n) \\ u^{n+1} = u^n + \frac{\Delta t}{2} (F(t, u^n) + F(t + \Delta t, u^{(1)})) \end{cases} \quad (22)$$

The superscripts  $n$  and  $n + 1$  denote consecutive time steps and the index 1 denotes an intermediate value. The field contribution on the right hand side of Eq.(12) is treated as a source term which is handled as in [18]. There is a time derivative part in the source term and we follow [19] and calculate it as  $\dot{s}_t = (s_t - s_{t-\Delta t})/\Delta t$  for the first step of Heun's method and use the value of the source term calculated in the intermediate step  $s_{t+\Delta t}^*$  to determine the time derivative in the second step, ie,  $\dot{s}_t = (s_{t+\Delta t}^* - s_t)/\Delta t$ .

Eq.(11) is rewritten as four first order equations as below (Eqs.(23) to (26)) and solved using Lax-Friedrichs scheme. We define  $\Psi_2 = \frac{\partial \phi}{\partial r}$  and  $\Psi_3 = \frac{\partial \phi}{\partial z}$  and

$$\Psi_1 = \frac{\partial \phi}{\partial t} \quad (23)$$

$$\frac{\partial \Psi_1}{\partial t} = \frac{\partial \Psi_2}{\partial r} + \frac{1}{r} \Psi_2 + \frac{\partial \Psi_3}{\partial z} - \frac{\partial V(\phi, T)}{\partial \phi} \quad (24)$$

$$\frac{\partial \Psi_2}{\partial t} = \frac{\partial \Psi_1}{\partial r} \quad (25)$$

$$\frac{\partial \Psi_3}{\partial t} = \frac{\partial \Psi_1}{\partial z} \quad (26)$$

The implementation of the scheme is as follows. When we have a 1D non-linear hyperbolic equation of the form

$$\frac{\partial u}{\partial t} + \frac{\partial f(u)}{\partial x} = 0 \quad (27)$$

the finite difference form given by the Lax Friedrichs scheme is

$$u_i^{n+1} = \frac{1}{2}(u_{i+1}^n + u_{i-1}^n) - \frac{\Delta t}{2\Delta x}(f(u_{i+1}^n) - f(u_{i-1}^n)) \quad (28)$$

The superscript  $n$ ,  $n+1$  denotes the time steps separated by  $\Delta t$  and the subscripts  $i-1$ ,  $i$  and  $i+1$  denote points in space separated by  $\Delta x$ . This scheme is first order accurate and suffers from numerical dissipation problem. In our case, this scheme along with a small dissipation term in the field evolution Eq.(24) at the initial times of the evolution seems to work well, as a first step. If the effective potential rapidly changes due to the change in temperature profile, the field could have large oscillations but we expect that in the presence of a medium which is coupled to the Polyakov loop field, this change will be smoother. The dissipation term, in a way, takes care of this coupling. The dissipation term is space dependent with its magnitude proportional to the magnitude of the Polyakov loop field. Hence it is small at the edges and does not hinder the expansion. This term is also gradually decreased to zero after a few time steps since as the temperature profile expands, the field profile seems to stabilize and do not oscillate rapidly. The surface term starts to affect the velocity build up only later in the evolution and hence this also makes sure that the surface effects are not affected by the dissipation term. If indeed there are large oscillations in the field, this scheme along with KT cannot handle the numerical simulation. Even with no oscillations, numerical instabilities develop at later times ( $> 15$  fm) at the boundary because of the source term and a better scheme for the scalar field evolution may improve this.

To summarize the numerical implementation, we use an initial Gaussian energy density profile to calculate the corresponding pressure, temperature and Polyakov loop field profiles. We assume zero initial velocity of the fluid and also  $\frac{d\phi}{dt} = 0$ . Using the initial temperature and  $\phi$  profiles, Eq.(11) is advanced by a time step. The energy-momentum tensor of the field

is calculated and Eq.(12) is advanced by a time step using KT scheme and a second order RK method. Energy density, pressure, velocity and temperature of the fluid are calculated from the new  $T_{fluid}^{\mu\nu}$  and the new temperature profile is used to evolve Eq.(11) again.

#### IV. RESULTS AND DISCUSSIONS

We study the development of flow with time in central and non-central initial conditions. The radial flow velocity and momentum anisotropy are defined as in [20]. The average radial flow velocity is given by

$$\langle v_r \rangle = \frac{\langle \gamma \sqrt{v_x^2 + v_y^2} \rangle}{\langle \gamma \rangle} \quad (29)$$

The angular brackets denote energy density weighted averages. The momentum anisotropy is given by

$$\epsilon_p = \frac{\langle T^{xx} - T^{yy} \rangle}{\langle T^{xx} + T^{yy} \rangle} \quad (30)$$

We see that the presence of the surface tension slows down the buildup of radial flow velocity as well as momentum anisotropy. It can be easily understood using Eq.(12). As the fluid expands the gradient energy of the field increases as a function of surface area, so the fluid has to do work to compensate for this. If we plot the velocity profile of the fluid, we see that the fluid slows down near the surface thereby slowing down the build up of radial flow velocity. Figure 3 shows the velocity profiles with and without surface tension. The dot-dashed curve represents the surface tension (gradient energy of  $\phi$  field). Since this value is very small, it is magnified by a factor of 10 here. One can see here that the fluid velocity slows down near the surface. Even though it picks up outside the surface, the energy density there is negligible to contribute to the flow.

Figures below show the evolution of the ratio of radial flow velocities with and without the order parameter field. We used 3 different widths for the spherically symmetric Gaussian profiles and 3 different values for the maximum energy density.

Figures 4(a), 4(b) and 4(c) show the evolution of radial flow at widths 2, 3 and 4 fm respectively, the three curves in each corresponding to three values of maximum energy densities. As expected, the suppression of radial flow decreases with increase in size. This is

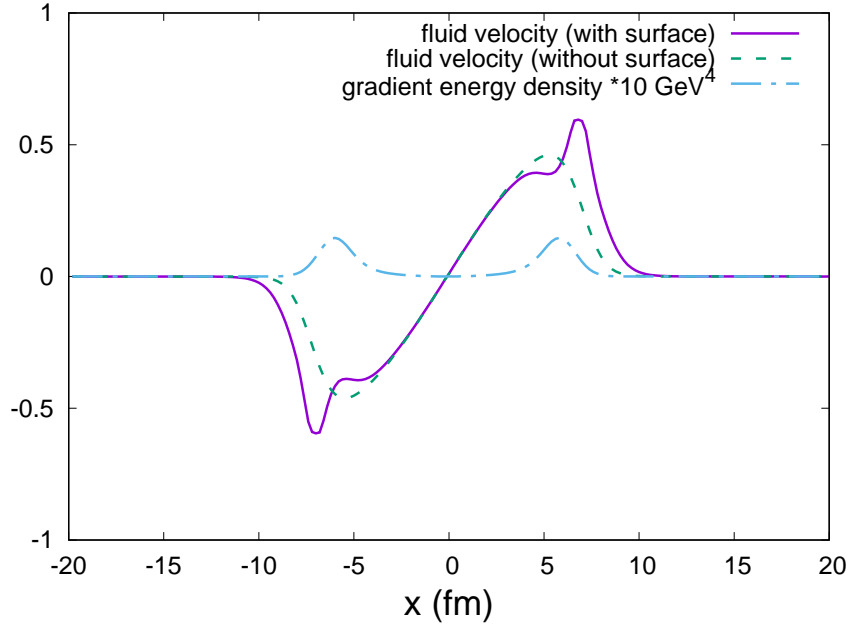


FIG. 3. Velocity profile along x-axis with (the continuous curve) and without (the dashed curve) surface tension at 2 fm/c. The dot-dashed curve represents the gradient energy contribution from the Polyakov loop field and is magnified by a factor 10 here.

explained by the fact that as size increases the ratio of surface area to volume decreases and the flow build up or the velocity build up which is a volume effect becomes stronger faster than the surface tension effect. Figures 5(a), 5(b) and 5(c) show the evolution of radial flow at maximum initial energy densities 2, 3, 4 GeV/fm<sup>3</sup> respectively. The three curves are the results for 3 different widths. Again, as initial energy density increases, the surface tension effect decreases since with increase in energy density, the pressure of the plasma increases faster than the surface energy and this strengthens the radial flow. What is of the most interest here is the percentage of suppression. At 15 fm/c, or an initial radius of 2 fm and an initial energy density 2 GeV/fm<sup>3</sup> gives a suppression as large as 40%. It gradually decreases with increase in size and energy, but there is a 5% suppression even at 4 fm and 4 GeV/fm<sup>3</sup>.

Similar results are seen in the development of momentum anisotropy as well. Figures 6(a), 6(b) and 6(c) show the evolution of momentum anisotropy with the minor axis of the ellipsoid 2 fm and the major axis 3, 4 and 5 fm respectively. It is interesting to note here that, when the major axis increases from 3 fm to 5 fm, the suppression of the momentum anisotropy decreases from 25% to 20% only, for  $\epsilon_{max} = 2$  GeV. This is because even though

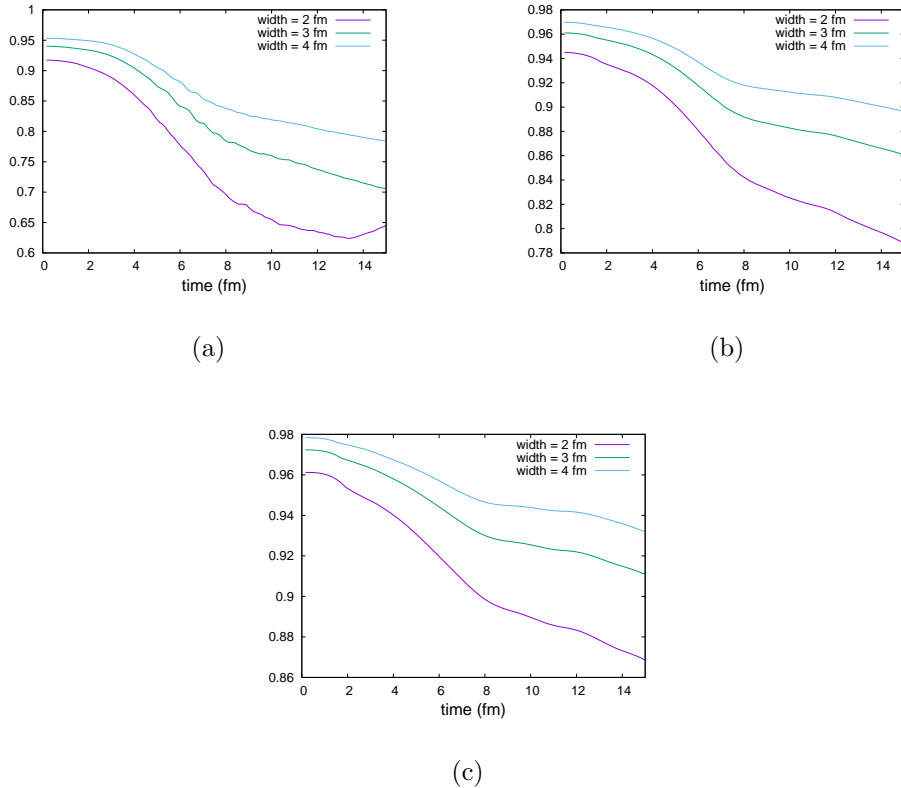


FIG. 4. Evolution of the ratio of radial flow with and without phase boundary effect. Figures (a), (b) and (c) show the evolution of radial flow for spherically symmetric Gaussian initial conditions with maximum energy values 2, 3 and 4 GeV/fm<sup>3</sup> respectively. The three curves in each case show the evolution for different sizes of the Gaussian.

an increase in major axis increases the size of the system, it also increases the anisotropy. This result also indicates that the effect of the phase boundary will be reflected in the development of elliptic flow.

## V. SUMMARY AND OUTLOOK

We introduce a new way of studying the effect of the presence of a surface in hydrodynamic evolution by coupling it to the order parameter field evolution. Polyakov loop model with a weak first order transition and no quarks is used for the equation of state of the fluid as well as the equation of motion of the order parameter field, whose gradient energy represents the phase boundary. The results show that even in the presence of a weak first order transition, the surface tension at the phase boundary tends to slow down the expansion. This effect is stronger when the system size is small or if the initial energy density of the

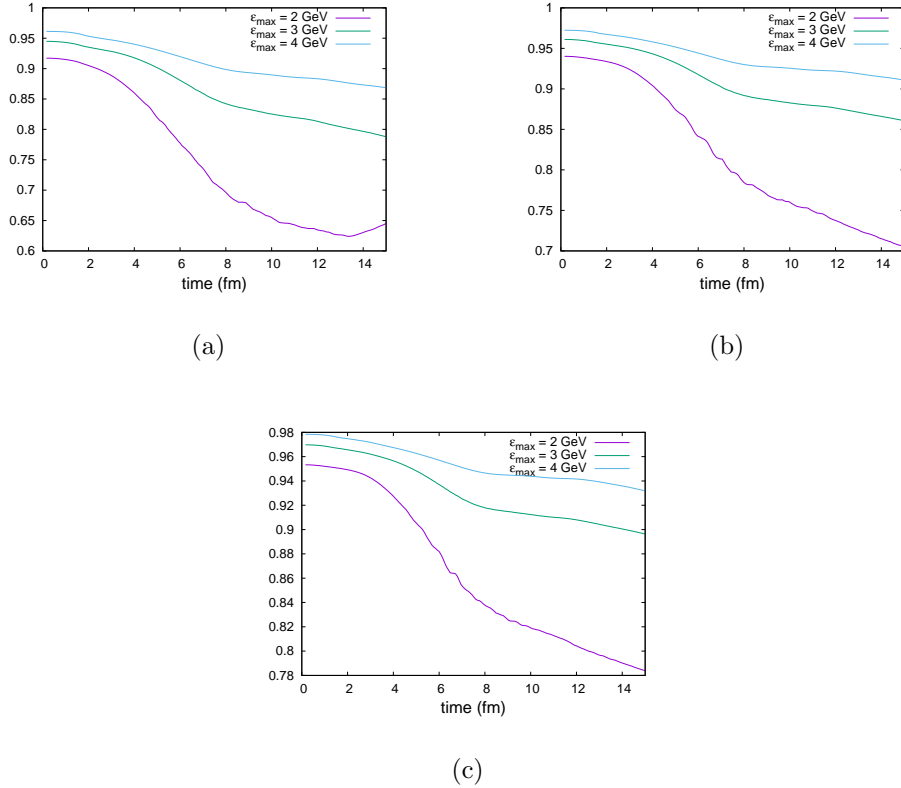


FIG. 5. Evolution of the ratio of radial flow with and without phase boundary effect. Figures (a), (b) and (c) show the evolutions for 3 different sizes of the Gaussian - 2, 3 and 4 fm respectively with 3 curves in each case showing the energy dependence as indicated in the figures.

system is small.

Even in case of a cross over transition, there will be a non-zero gradient energy at the phase boundary. We wrote down an effective potential with a small explicit symmetry breaking and a cross over transition and checked the effects of the gradient term on hydrodynamics. The gradient term was small to make any visible effects in our case. But if the cross over is sharper, the flow may be affected. We also tried to study the effect of a stronger first order transition by scaling the effective potential to increase the barrier height between the two states at transition temperature. A higher barrier height means higher surface energy and as a result more resistance to expansion. With our parametrisation, we found that the effect of this on flow was smaller since the higher barrier height made the surface sharper and as a result the fluid started feeling its presence only later. But we expect a stronger suppression at later times. In order to study it more accurately, one needs a more realistic model of strong first order transition as well as a more accurate numerical method

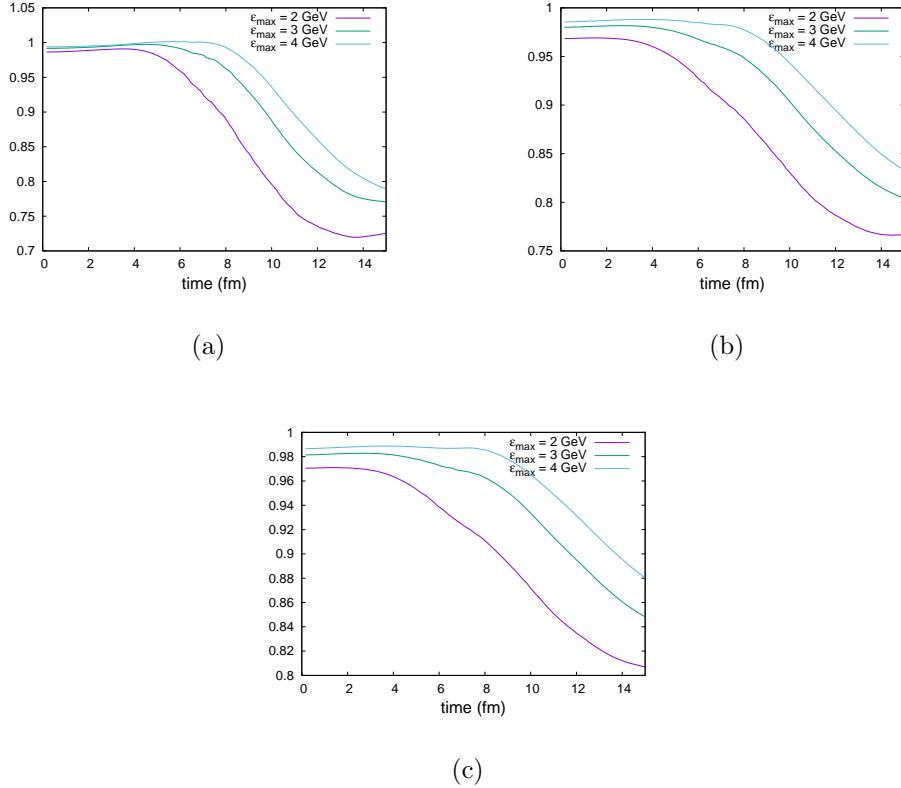


FIG. 6. Evolution of ratio of momentum anisotropy with and without phase boundary. Figures (a), (b) and (c) have major axes 3 fm, 4 fm and 5 fm respectively for the ellipsoid when the minor axis is 2 fm for all. The three different curves show the evolution for 3 different maximum energy density values as indicated in the figures for the initial Gaussian energy density profiles.

for solving the order parameter equation of motion so that the system can be evolved for longer times.

We have shown that the gradient energy in the order parameter field at a phase boundary affects collective flow. This effect is more for smaller systems and at lower energies in presence of a weak first order transition. The model studied here assumes a baryon less fluid. First order transition is expected to occur at high baryon densities and it will be interesting to study this effect including the flow of baryons in a more realistic case. One should also address the presence of hadrons using a better equation of state. In low energy collisions, the system is expected to spend some time in hadronic state before freeze out and it will be interesting to see the effect of this in the suppressed fluid flow. But we believe that our study is an effective way to capture the dynamics of an expanding fluid with a phase boundary. The complex Polyakov loop field evolution in an effective potential can also



explain the dynamics of center domains,  $Z(3)$  walls and strings [7–9] and we believe that our formulation with appropriately modified order parameter field equations and equations of state could also study the dynamics of  $Z(3)$  walls and strings in a quark gluon fluid - the effect of topological structures on flow and vice versa.

## ACKNOWLEDGMENTS

We are very grateful to Andrey Khvorostukhin for detailed discussions of the numerical techniques, suggesting KT scheme for the conservation equations as well as for his comments on the manuscript. We also thank Ajit Srivastava for very useful comments and suggestions on this work. We thank Shreyansh S. Dave for his useful comments on the manuscript.

- 
- [1] Y. Aoki et al., *Nature* **443**, 675 (2006).
  - [2] J. Luecker et al., arXiv:1308.4509.
  - [3] P. Senger, *Eur. Phys. J. A* **52**, 217 (2016).
  - [4] Johann M. Heuser, *Nucl. Phys. A* **904**, 03001 (2011).
  - [5] Pasi Huovinen, *Int. J. of Mod. Phys. E* **22**, 1330029 (2013).
  - [6] Piotr Bozek, *Acta Phys. Polon. B* **43**, 689 (2012).
  - [7] Uma Shankar Gupta, Ranjita K. Mohapatra, Ajit M. Srivastava, Vivek K. Tiwari, *Phys. Rev. D* **86**, 125016 (2012).
  - [8] Ranjita K. Mohapatra, Ajit M. Srivastava, *Phys. Rev. C* **88**, 044901 (2013)
  - [9] Uma Shankar Gupta, Ranjita K. Mohapatra, Ajit M. Srivastava, Vivek K. Tiwari, *Phys. Rev. D* **82**, 074020 (2010).
  - [10] Ranjita K. Mohapatra, Hiranmaya Mishra, *Phys. Rev. D* **95**, 094014 (2017).
  - [11] V. V. Skokov, D. N. Voskresensky, *Nucl. Phys. A* **828**, 401 (2009).
  - [12] R. D. Pisarski, *Phys. Rev. D* **62**, 111501(R) (2000).
  - [13] A. Dumitru and R. D. Pisarski, *Phys. Lett. B* **504**, 282 (2001) doi:10.1016/S0370-2693(01)00286-6 [hep-ph/0010083].
  - [14] A. Dumitru and R. D. Pisarski, *Nucl. Phys. Proc. Suppl.* **106**, 483 (2002) doi:10.1016/S0920-5632(01)01754-6 [hep-lat/0110214].

- [15] Jorgen Randrup, Phys. Rev. **D 55**, 1188 (1997).
- [16] A. Kurganov, E. Tadmor, J. Comput. Phys. **160** 241–282 (2000).
- [17] Bjorn Schenke, Sangyong Jeon, Charles Gale, Phys. Rev. **C 82**, 014903 (2010).
- [18] R. Naidoo and S. Baboolal, Future Gener. Comput. Syst. 20, 465 (2004).
- [19] Bjorn Schenke, Sangyong Jeon, and Charles Gale, Phys. Rev. Lett. **106**, 042301 (2011).
- [20] Peter F. Kolb, Josef Sollfrank, Ulrich Heinz, Phys. Rev. **C 62**, 054909 (2000).